Chinese Journal of
POLYMER SCIENCE

RESEARCH ARTICLE

https://doi.org/10.1007/s10118-023-2901-y
Chinese J. Polym. Sci. **2023**, *41*, 1115–1122

A Facile Strategy to Enhance the Formation of Stereocomplex Crystallites in Poly(L-lactic acid)/Poly(D-lactic acid) Blend with High Molecular Weights

Chan-Na Zhong[a], Ya-Dong Liu[b*], Juan Tang[a], Wei-Shuo Chen[a], Shuang-Cheng Li[a], Jun Shao[a,c*], and Hao-Qing Hou[a,c]

[a] *College of Chemistry & Chemical Engineering and Nanofiber Engineering Center of Jiangxi Province, Jiangxi Normal University, Nanchang 330022, China*
[b] *Key Laboratory of Polymer Ecomaterials, Changchun Institute of Applied Chemistry, Chinese Academy of Sciences, Changchun 130022, China*
[c] *National Engineering Research Center for Carbohydrate Synthesis/Key Lab of Fluorine and Silicon for Energy Materials and Chemistry of Ministry of Education, Jiangxi Normal University, Nanchang 330022, China*

Electronic Supplementary Information

Abstract Blending of poly(levorotatory-lactic acid) (PLLA) and poly(dextrorotatory-lactic acid) (PDLA) produces the stereocomplex crystallites (PLA SC), which present higher melting temperature and mechanical properties than that of neat PLLA or PDLA. However, in the PLLA/PDLA blends with higher molecular weights, the phase separation occurs and the SC exhibits weak memory after melting, which lead to a small amount of SC together with a large amount of homochiral crystallites (HC) develop during crystallization from the melt. In this study, a small content of graphite oxide was blended with PLLA and PDLA to form ternary blends, and it was exciting to find that the formation of SC was enhanced gradually with the content of graphite oxide. The SC exclusively developed when 2 wt% graphite oxide was incorporated into the PLLA/PDLA, and the crystallinity with ~50% was received even during fast cooling from the melt (−50 °C/min). The acceleration formation of SC was speculated due to the interaction between PLA molecular chains and the hydroxyl groups on the surface of graphite oxide and the obstruction of proliferation of graphite oxide.

Keywords Poly(lactic acid) stereocomplex; Graphite oxide; Crystallization behavior; Melt memory

Citation: Zhong, C. N.; Liu, Y. D.; Tang, J.; Chen, W. S.; Li, S. C.; Shao, J.; Hou, H. Q. A facile strategy to enhance the formation of stereocomplex crystallites in poly(L-lactic acid)/poly(D-lactic acid) blend with high molecular weights. *Chinese J. Polym. Sci.* **2023**, *41*, 1115–1122.

INTRODUCTION

When coming to the Twenty-First Century, the resource crisis and environmental pollution issues encouraged the rapid development of bio-derived and biodegradable polymers as alternatives to conventional petroleum-derived and non-biodegradable polymers. Poly(lactic acid) (PLA) is regarded as one of the promising environmentally friendly and bio-based material, due to its renewable, biodegradable, biocompatible and excellent mechanical properties.[1] Since the lactic acid has two configurations, the crystallizable PLAs compose two kinds of isomer polymers, *i.e.*, poly(levorotatory-lactic acid) and poly(dextrorotatory-lactic acid), which are coded as PLLA and PDLA, respectively. Blending PLLA with PDLA, a novel PLA stereocomplex crystallites (SC) fabricated.[2] The SC exhibited higher melting temperature (~250 °C),[3–5] faster crystallization rate, superior mechanical performance and better hydrolysis resistance than that of PLLA or PDLA homochiral crystallites (HC).[6–8] Notwithstanding, it is gloomy that the SC exclusively develop in the PLLA/PDLA blends with relative lower molecular weights (≤40 kg/mol).[3,9,10] However, the PLLA/PDLA with low molecular weights has poor mechanical properties, and promoting PLA SC material with high molecular weights (>60 kg/mol) is great significance for practical application. For the PLLA/PDLA blends with higher molecular weights, the SC together with HC developed, which was called as "microphase separation" and reduced the heat deformation temperature and mechanical strength of PLLA/PDLA.[11,12] Many approaches have been proposed to promote the formation of SC in the PLLA/PDLA blends with higher molecular weights, such as preparation of stereocomplex crystallites by solvent mixing for longer time[9] or at higher temperature,[13] repeated casting,[14] adding nucleating agent,[15–20] annealing at proper temperature,[21] drawing at a specific temperature and condition,[22–24] varying the structure of PLA,[5,25,26] blending at a proper temperature (among the melting temperature of HC and SC),[27–30] streocomplexation at supercritical fluid,[31] exerting

* Corresponding authors, E-mail: ydliu26@ciac.ac.cn (Y.D.L.)
E-mail: jun.shao@jxnu.edu.cn (J.S.)

Received August 19, 2022; Accepted November 14, 2022; Published online December 29, 2022

shearing[32,33] on the melt and incorporating the third component,[34–37] *etc*. Most of the above methods enhanced the formation of SC effectively. However, another negative factor which also limit the application of the SC on a large scale, *i.e.*, the SC exhibited weak "melt memory effect", and a large amount of HC against SC develop after melting crystallization in the PLLA/PDLA specimens with high molecular weights. Adding nucleate agent is a simple but efficient approach to accelerate crystallization rate and promote SC formation of PLLA/PDLA blends as it can be conveniently realized by melting processing. Notwithstanding, lots of the reported nucleators can not only nucleate the SC formation but also HC.[16–19] Therefore, it is a significant work to produce a stable and high content of SC during melted blending, and which could not only improve the mechanical properties, but also facilitate the processing and engineering application. In this paper, a small amount of graphite oxide was added into PLLA/PDLA mixture, and the analysed data revealed that the SC exclusively developed during different crystallization conditions. This investigation would be helpful for preparation the high content of SC in the PLLA/PDLA blends with high molecular weights.

EXPERIMENTAL

Materials

The PLLA REVODE190 (weight average molecular weight (M_w) was 130 kg/mol, and molecular weight distributions (PDI) was 1.6 (determined by gel permeation chromatography), were kindly supplied by Zhejiang Hisun Biomaterials Co., Ltd. (China). The PDLA D120 (M_w and PDI were 178 kg/mol and 1.7, respectively) was bought from Total-Corbion. The graphite oxide (KNG-21) was brought from Xiamen Knano Graphene Technology Co., Ltd. (China), the weight percentage of oxygen atom of the graphite oxide was ~35 wt%. Graphite powder was purchased from Aladdin, with the average size of ~325 mesh. After blending with PLLA and PDLA, the average sizes of graphite oxide and graphite are ~21 and ~25 μm, respectively.

Preparation the PLLA/PDLA/Graphite Oxide Blends

The PLLA/PDLA/graphite oxide ternary blends with different weight ratios of were melting blended by using a torque rheometer internal mixer (XSS-300, Shanghai Kechuang Rubber Plastic Mechanical Equipment Co., Ltd., China), the mixing was carried out at a temperature of 230 °C for 8 min, and the rotation speed of rotator was fixed at 60 r/min. The weight ratio of PLLA/PDLA was fixed at 50/50 in this investigation. The weight percentage of graphite oxide was set as 0%, 0.5%, 1%, 1.5% and 2%, respectively in the blends, and the specimens were separately coded as 0%, 0.5%, 1%, 1.5% and 2%. For comparison, the PLLA/PDLA with 2% graphite was also prepared at the same condition.

Characterizations

Wide angle X-ray diffraction (WAXD) measurements were carried out on a customized micro-focus WAXD system. A focused Cu Kα X-ray source (GeniX^{3D}, Xenocs SA, France), generated at 50 kV and 0.6 mA, was employed in this setup. The two-dimensional (2D) WAXD patterns were collected by a semiconductor detector with a resolution of 487 pixels × 195 pixels (pixel size=172 μm) (Pilatus100 K, DECTRIS, Swiss) at a sample-to-detector distance of 20.8 mm. The fid2D software was employed to analysis the 2D patterns and to produce the one-dimensional WAXD data.

Fourier transform infrared (FTIR) spectra were recorded using a Bio-Rad Win-IR instrument in the range of 4000–500 cm^{-1} (Thermo Scientific, Nicolet 6700). The reflection mode was applied during measurement. All spectra were recorded by averaging 16 scans at a resolution of 4 cm^{-1} and were baseline corrected.

Thermal properties of samples were performed on the differential scanning calorimeter (DSC, Q20, TA, American) apparatus under nitrogen atmosphere. The temperature and heat flow were calibrated with standard indium (T_m=156.6 °C, ΔH_m=28.5 J/g). For the non-isothermal crystallization, the specimens were heated from 20 °C to 250 °C at a rate of 10 °C/min, and hold at 250 °C for 1 min. After that, the specimens were cooled at a speed of 50 °C/min to room temperature, and the DSC measurements were repeated heating and cooling for four times to detect the crystallization behavior of the specimens. The crystallinity of SC (X_{SC}) and HC (X_{HC}) were calculated from the following equations, respectively.

$$X_{SC}\ (\%) = \frac{\Delta H_{SC}}{\omega_{PLA} \times 142\ \mathrm{J/g}} \times 100\% \quad (1)$$

$$X_{HC}\ (\%) = \frac{\Delta H_{HC}}{\omega_{PLA} \times 93\ \mathrm{J/g}} \times 100\% \quad (2)$$

where the ΔH_{SC} was the melting enthalpy of PLA SC in the specimen, which was calculated from the DSC curve, and 142 J/g was the reported enthalpy value for 100% crystallized of SC.[38] The ΔH_{HC} was the melting enthalpy of HC, and the ΔH_{HC} value for 100% crystallized HC was reported as 93 J/g.[39] The ω_{PLA} was the weight percentage of the PLA (PLLA+PDLA) in the PLLA/PDLA/graphite oxide blend.

RESULTS AND DISCUSSION

Crystallization of the PLLA/PDLA/Graphite Oxide Specimens

After blending at 230 °C for 8 min, and cooled to room temperature in the air, WAXD profiles of the PLLA/PDLA/graphite oxide blends are presented in Fig. 1. It is known that the diffraction peaks located at 16.9° and 19.1° were attributed to the 110/200 and 203 plane of the PLA α (or α') crystallites (HC), respectively,[40–42] and the diffractions at 12.1°, 21.0° and 24.0° were separately assigned to 110, 300/030 and 220 reflections of PLA SC.[43–45] In the specimen of 0%, the diffraction peaks located at 12.1°, 16.9°, 19.1° and 21° were observed, indicating that both PLA HC and SC were produced. In the 0.5% specimen, both the intensity of diffractions assigned to HC and SC increased, but the intensity ratio of the 16.9°/12.1° (I_{HC}(200/110)/I_{SC}(110)) reduced compared with that value of the 0%, which implied that more content of SC produced in the 0.5% specimen. The diffraction peaks belonged to SC enhanced gradually, while the diffractions assigned to HC reduced and vanished as further increasing the content of graphite oxide. For the specimens of 1.5% and 2%, only diffractions assigned to SC were observed, suggesting that the graphite oxide at this content could promote the SC formation exclusively.

The FTIR spectra of the ternary samples are shown in Fig. 2. The signals at 909 and 921 cm^{-1} are the characteristic absorp-

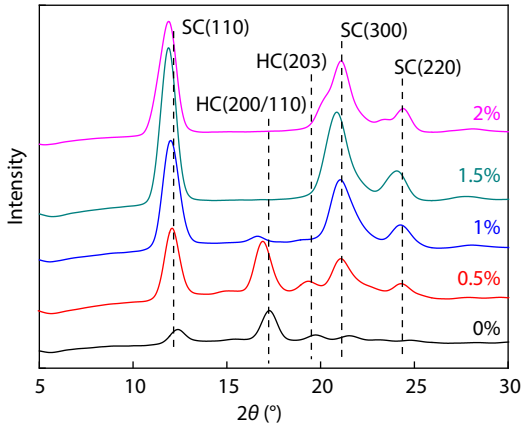

Fig. 1 WAXD patterns of PLLA/PDLA/graphite oxide specimens.

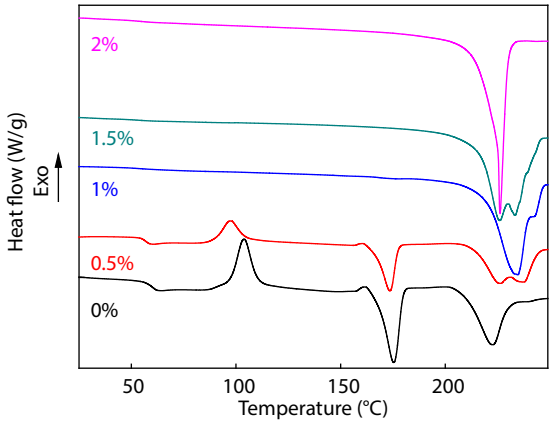

Fig. 3 DSC curves of the PLLA/PDLA/graphite oxide specimens.

tion bands of PLA SC (3_1 helix) and α (α') crystallites (10_3 helix), respectively.[22,42] For the specimen of 0%, two weak absorb bands were separately observed at 909 and 921 cm^{-1}. With the increment of graphite oxide, the intensity of signals at 909 cm^{-1} enhanced, while the absorption at 921 cm^{-1} reduced progressively and disappeared, which implied that the content of SC increased, and the content of HC reduced with more content of graphite oxide incorporated into the PLLA/PDLA matrix.

The DSC curves of the specimens are exhibited in Fig. 3, and the data calculated from DSC curves were list in Table S1 (in the electronic supplementary information, ESI). For the 0% sample, a glass transition temperature (T_g) was found at 60 °C, and a cold crystallization peak (T_{cc}) appeared at 104 °C. The melting temperature of HC (T_{HC}) was observed at 175 °C, and the melting temperature of PLA SC (T_{SC}) was found at 222 °C. After graphite oxide was incorporated into PLLA/PDLA, the signals assigned to T_g, T_{cc} and T_{HC} gradually declined, and became not obvious, while the signals belonged to the melting of PLA SC turned apparently with more content of graphite oxide. Double melting peak was found around at 230 °C when the content of graphite oxide ranged from 0.5% to 1.5 %. In the specimen of 1.5%, only the endothermic signals assigned to SC were observed, and the melting enthalpy (ΔH_{SC}) was 108.9 J/g (for the total melting enthalpy of the two peaks,

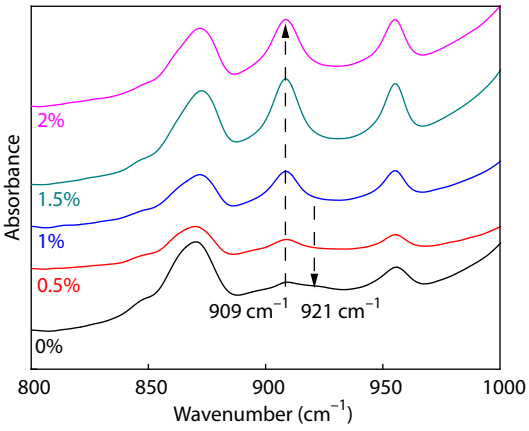

Fig. 2 FTIR spectra of the PLLA/PDLA/graphite oxide specimens.

Table S1 in ESI). Further increasing the content of graphite oxide (2%), the double melting peak disappeared, and the ΔH_{SC} reduced. Combined with the second DSC heating curves (the results are listed in Table S1 in ESI and Fig. 4), the double melting peaks appeared in the 0.5%, 1% and 1.5% specimens, and two possibilities could be resulted to the multiple melting behaviors, the one is that, the imperfect crystallites developed during mixing in the mixer, and they were melted at the lower temperature. Then, the molecular chains recrystallized and formed perfect crystallites at a fast rate during heating. The other possibility is that, the crystallites with different perfection developed during the mixing, the imperfect crystallites were melted at the lower temperature, the perfect crystallites were melted at the higher temperature.[3,4]

All the WAXD, FTIR and DSC results revealed that incorporating graphite oxide into PLLA/PDLA facilitated the formation of SC, and inhibited the formation of HC. The SC exclusively developed in the PLLA/PDLA/graphite oxide ternary blends when the graphite oxide content was 1.5%.

The Memory Effect of PLLA/PDLA/Graphite Oxide Melted Specimens

Liu *et al.*,[27] Bao *et al.*,[28] and Bai *et al.*[29,30,46] reported that the SC could exclusively develop in the PLLA/PDLA blends with high molecular weights when blending at a proper temperature (between the T_{HC} and T_{SC}). However, the weak melt memory effect of SC would produce a large amount of HC during the subsequently melting crystallization. In order to observe the memory behavior of SC from the melt, the repeated heating-cooling process of the PLLA/PDLA/graphite oxide specimens were examined, and selected DSC results are shown in Fig. 4. The calculated data from the DSC are listed in Table S1 (in ESI). For the second heating of the 0% (Fig. 4a), the T_g, T_{cc} appeared at higher temperature than that of the first heating, the melting enthalpy of HC (ΔH_{HC}) became larger (increased from 36.1 J/g to 44.0 J/g), and the ΔH_{SC} became smaller (declined from 44.9 J/g to 14.2 J/g) than those values of the first heating. Melting for more times, the ΔH_{HC} did not exhibit obviously divergences, and the ΔH_{SC} declined slightly. The higher value of ΔH_{SC} in the first DSC heating should be ascribed to the blending temperature was 230 °C, and the melted isomer polymer chains could form SC at this temperature. After heating to 250 °C, all

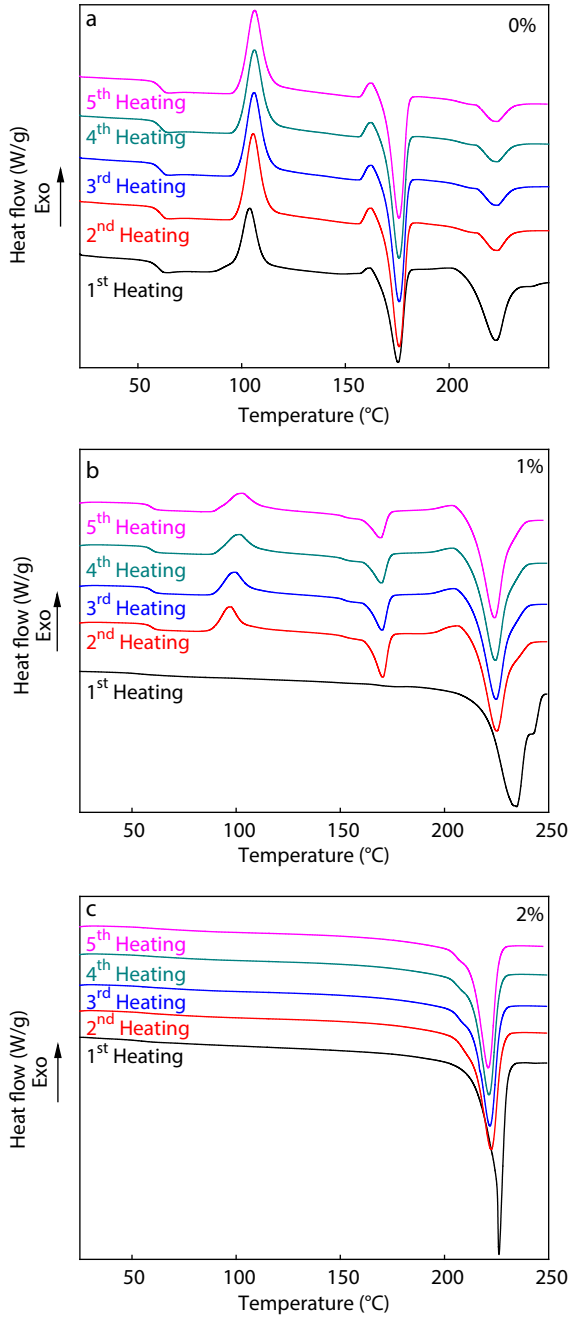

Fig. 4 The repeated heating DSC curves of the PLLA/PDLA/graphite oxide specimens: (a) 0%, (b) 1%, and (c) 2%.

the crystallites were melted completely, and homogenous melt were produced. Thus, the homochiral polymers could aggregate together to form HC conveniently. This result indicated that the SC exhibited weak melt memory effect in the PLLA/PDLA binary blend. In the case of 1% specimen (Fig. 4b), the cold crystallization peak appeared, the signal assigned to HC became obvious, and the ΔH_{SC} declined significantly (from 93.1 J/g to 56.5 J/g) for the second heating. Melting for more times, the T_g and T_{cc} did not vary distinctly, ΔH_{HC} declined gradually, and the ΔH_{SC} fluctuated at 63.0 J/g. For the specimen of 2% specimen (Fig. 4c), both the T_{SC} and ΔH_{SC} did not vary obviously for all the heating curves, the SC produced rapidly even during the fast cooling (the cooling curves are listed in Fig. S1 in ESI), and no cold crystallization peak and melting signals assigned to HC were detected on the subsequently heating. As more content of graphite oxide added into the PLLA/PDLA matrix, the signals assigned to cold crystallization declined, the T_{cc} and the X_{HC} decreased distinctly, while the X_{SC} increased (the repeated heating-cooling DSC of 0.5% and 1.5% specimens were exhibited in Fig. S2 and Fig. S3 in ESI, respectively, and their DSC data were also listed in Table S1 in ESI). These results revealed that incorporating graphite oxide enhanced the melt memory of SC significantly. For the specimen of 2%, the crystallization enthalpy (ΔH_c) was ~67 J/g for the repeated heating and fast cooling process, (the X_c was 48% according to Eq. 1), these results hinted that the samples would in favor of formation SC during fast cooling.

There exists another possibility that, a small amount of SC was not melted completely in the PLLA/PDLA/graphite oxide specimens, and these remained SC acted as nucleate agents and accelerated the formation of SC. In order to eliminate this possibility, all the specimens were melted for 250 °C for 1 min, and then, they were immediately quenched in liquid nitrogen for 10 min. The WAXD profiles of these quenched specimens are displayed in Fig. S4 (in ESI), and no diffraction peak was observed in all of the specimens, indicating that no crystallites were remained after melting at 250 °C for 1 min. In addition, the 2% specimen was melted for 255 °C for 3 min, and was fast cooled to 170 °C, and the result indicated that the SC solely developed rapidly during crystallization (see Fig. S5 in ESI). After melting at 250 °C for 1 min, and quenched in liquid nitrogen, the subsequently heating DSC curves of the specimens were measured and presented in Fig. 5. As the content of graphite oxide increasing in the specimen, the T_g reduced slightly, and the T_{cc} depressed obviously. For the 0% and 0.5% specimens, the HC together with SC developed during crystallization, and the formation of HC and SC could compete with each other, leading to the higher T_{cc}. In the cases of 1.5% and 2% specimens, a large amount of PLA SC produced at a lower temperature.[47] The T_{HC} and ΔH_{HC} declined, while the ΔH_{SC} increased as more content of graphite oxide incorporated into the PLLA/PDLA. For the 2%, PLA SC exclusively de-

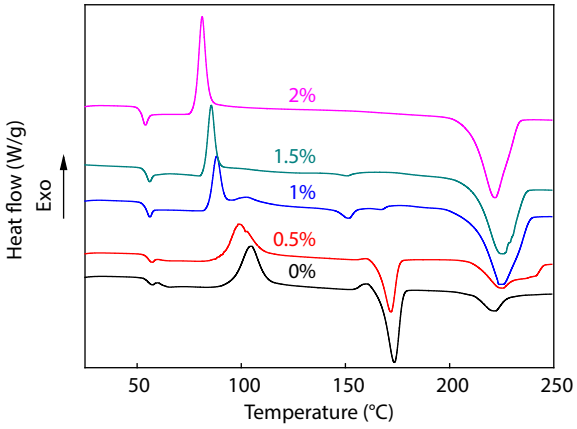

Fig. 5 DSC curves of melt-quenching PLLA/PDLA/graphite oxide specimens.

veloped during crystallization.

When these quenched specimens were annealed at 100 °C for 30 min, the SC also exclusively develop in the 2% specimen (Fig. 6). These results revealed that the addition of graphite oxide inhibited the development of HC, and accelerated the formation of SC. Consequently, the melt memory effect of SC was enhanced with increasing the content of graphite oxide.

From Fig. 3, only SC developed when the content of graphite oxide was 1.5%, but from the results of Figs. 4, 5 and 6, the SC exclusively developed in the specimen of 2%, and the isothermal crystallization also attested that only SC developed in the 2% specimen (Figs. S6 and S7 in ESI). These differences would be due to the different heating history. Blending at 230 °C, parts of SC developed and remained in the specimen. The remained SC and the existence of graphite oxide acted as the nucleate agents, which facilitated the SC develop rapidly at higher temperature during the cooling process. Thus, the large amount of SC restricted the formation of HC. For the specimen annealed at 250 °C, all the crystallites were completely melted. In this situation, only the graphite oxide could facilitate the formation of SC, therefore, the SC exclusively developed with higher content of graphite oxide.

All the results in this investigation indicated that, incorporating a small amount of graphite oxide would enhance the formation of PLA SC. However, the T_{SC} in the specimen of 2% was slightly lower than that of 0% specimen after the repeated melting process (~2 °C). From the reported literatures,[15,18,48] the T_{SC}, in the specimens that SC was exclusively produced, were obviously lower than that PLLA/PDLA binary blends (~10 °C), the differences of T_{SC} for different specimens would be due to their discrepant crystallization mechanisms.

Mechanism for the Enhancement of Melt Memory Effect of SC

In order to clarify the mechanism of the enhancement the melt memory effect of SC after incorporating graphite oxide, the graphite with a similar size of graphite oxide was also blended with PLLA/PDLA as the same condition, and the DSC results are presented in Fig. S8 and Table S1 (in ESI, which was called as G-2%). From the DSC curves, it can be found that no crystallization

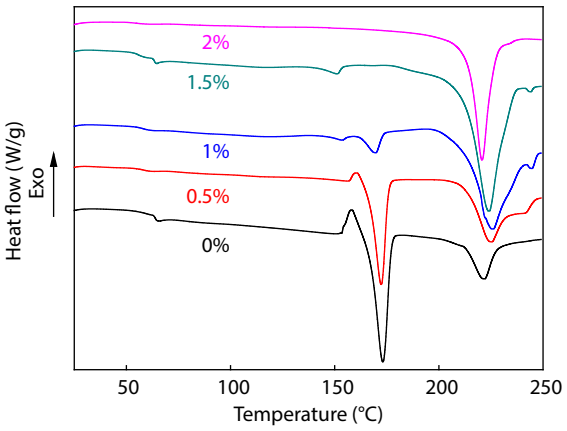

Fig. 6 DSC curves of the annealed (at 100 °C for 30 min) specimens after melt-quenching.

peak was detected during the fast cooling, and the ΔH_{HC} and ΔH_{SC} were similar with those values of PLLA/PDLA binary blend during the subsequently heating, which indicating that incorporating 2% graphite did not enhance the crystallization capacity of SC obviously. However, for the PLLA/PDLA/graphite oxide ternary blends, the WAXD, FTIR, DSC measurements all attested that the melting enthalpy of SC in the specimens was enhanced as the content of graphite oxide increased from 0.5% to 2%. As the size of graphite and graphite oxide was similar, the hydroxyls on the surface of graphite oxide should play critical roles for the formation of SC. Thus, it is rational to speculate that there should exist interaction between the hydroxyls on the surface of graphite oxide and the PLA molecular chains.

Zhang's investigation revealed that the formation of PLA SC was attributed to the CH_3--O═C hydrogen bond between isomer polymers.[49] Yang *et al*. and Li *et al*. found that the formation of hydrogen bonds between enantiomers is a prerequisite for SC generation.[50,51] During crystallization, the hydroxyl groups would interact with PLA molecular chains and formed hydrogen bond, and this interaction promoted the formation of SC.[48] In this study, the graphite oxide presented multi-layer structure, and the interlayer distance is ~8.035 Å according to the XRD in Fig. S9 (in ESI) and the Scherrer equation. In addition, lots of hydroxyls were on the surface of each layer. During crystallization from the melt, the PLA molecular chains would interact with the hydroxyl groups on the surface of the graphite oxide easily. The interaction could fix the PLA molecular chains on the surface of graphite oxide (Scheme 1) conveniently. This interaction and fixation could supply templates to absorb isomer polymers to arrange side by side alternately through hydrogen bond formation. Accordingly, the PLA SC developed preferentially under the template produced on the surface of graphite oxide.

In addition, the diffusion of the isomer molecular chains to the crystal growth front is another issue for the formation of SC. As the PLLA was not fully compatible with PDLA especially at high molecular weight specimens,[52,53] the PLA molecular chains with similar chair structures could segregate together and produced the PLLA-rich district and PDLA-rich district under the molten state, and which facilitate the formation of PLA HC during crystallization. Only the contact regions between PLLA-rich and PDLA-rich district could produce the SC. Thus, a large amount of HC and a small amount of SC developed during crystallize from the melt in the PLLA/PDLA binary blend. In the PLLA/PDLA/graphite oxide ternary blends, the diffusion and phase separation between isomer polymers was interrupted by the graphite oxide, as the graphite oxide was presented with a planar structure and a larger size than PLA molecular chains, which blocked the diffusion of molecular chains. Moreover, the stronger interaction between the graphite oxide and the PLA molecular chains also restricts the motivation of PLA molecular chains. Then, the enantiomeric PLA molecular chains in the PLLA/PDLA/graphite oxide specimens could interact and arranged alternatively easily.

Accordingly, the interaction between the hydroxyls on the surface of graphite oxide and the PLA molecular chains, and the interrupted diffusion could facilitate the formation of SC.

https://doi.org/10.1007/s10118-023-2901-y

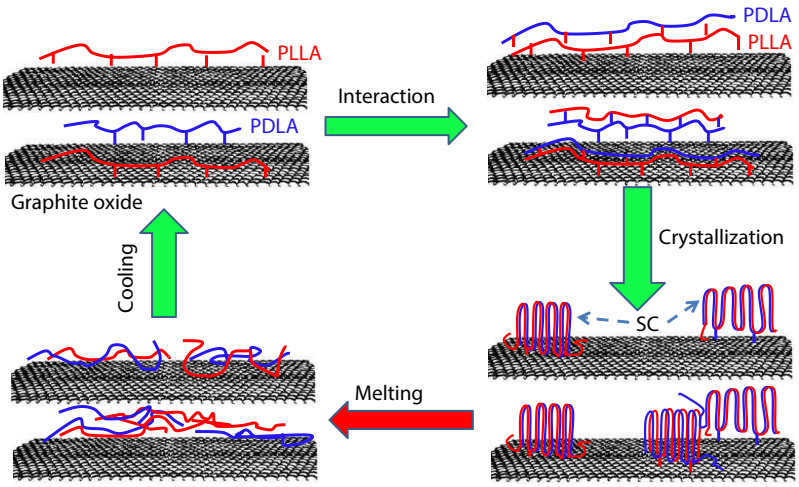

Scheme 1 Schematic illustration for the formation of PLA SC.

CONCLUSIONS

In this study, the PLLA/PDLA specimen with higher molecular weights was melt blended with a small amount of graphite oxide, after investigating the crystallization behavior on various approaches, the conclusions would be made as follows.

1. After melted blending and cooled to room temperature in the air, the WAXD, FTIR and DSC results indicated that, the content of SC increased, while the content of HC reduced and disappeared as the content of graphite oxide increased from 0.5% to 2%.

2. As the content of graphite oxide increased in the blend, the melt memory effect of SC enhanced gradually. For the PLLA/PDLA blend with 2% graphite oxide, the melt memory effect of SC almost kept constant in the repeated heating and cooling, and the X_c with ~50% was received even during the fast cooling.

3. The mechanism of promotion of SC could be due to the restricted interdiffusion of polymers under the existence layer structure of graphite oxide and specific interaction between the surface of graphite oxide and PLA molecular chains and segments.

This investigation provides a possibility that preparation the PLLA/PDLA blends with high content of SC with fast melt-processing.

Conflict of Interests

The authors declare no interest conflict.

Electronic Supplementary Information

Electronic supplementary information (ESI) is available free of charge in the online version of this article at http://doi.org/10.1007/s10118-023-2901-y.

ACKNOWLEDGMENTS

This work was financially supported by the National Natural Science Foundation of China (Nos. 51403089 and 21574060), the Major Special Projects of Jiangxi Provincial Department of Science and Technology (No. 20114ABF05100), the Project of Jiangxi Provincial Department of Education (No. GJJ170229), the China Postdoctoral Science Foundation (No. 2019M652282), the Postdoctoral Science Foundation of Jiangxi Province (No. 2018KY37), the Technology Plan Landing Project of Jiangxi Provincial Department of Education (No. GCJ2011-243), the Science Foundation for Excellent Young Scholars of Jiangxi Province (No. 20202ZDB01003), and the Science foundation of Jiangxi Province (No. 20202BAB203008).

REFERENCES

1 Pang, X.; Zhuang, X. L.; Tang, Z. H.; Chen, X. S. Polylactic acid (PLA): research, development and industrialization. *Biotechnol. J.* **2010**, *5*, 1125–1136.
2 Ikada, Y.; Jamshidi, K.; Tsuji, H.; Hyon, S. H. Stereocomplex formation between enantimoeric poly(lactides). *Macromolecules* **1987**, *20*, 904–906.
3 Shao, J.; Xiang, S.; Bian, X. C.; Sun, J. R.; Li, G.; Chen, X. S. Remarkable melting behavior of PLA stereocomplex in linear PLLA/PDLA blends. *Ind. Eng. Chem. Res.* **2015**, *54*, 2246–2253.
4 Hu, X. D.; Shao, J.; Zhou, D. D.; Li, G.; Ding, J. X.; Chen, X. S. Microstructure and melting behavior of a solution-cast polylactide stereocomplex: effect of annealing. *J. Appl. Polym. Sci.* **2017**, *134*, e46626.
5 Shao, J.; Sun, J. R.; Bian, X. C.; Cui, Y.; Li, G.; Chen, X. S. Investigation of poly(lactide) stereocomplexes: 3-armed poly(L-lactide) blended with linear and 3-armed enantiomers. *J. Phys. Chem. B* **2012**, *116*, 9983–9991.
6 Chen, L.; Tang S. C.; Xia, J.; Pu, W. L.; Li, R. Crystallization structures and thermal properties of high heat-resistance PLLA/PDLA blends. *Acta Polymerica Sinica* (in Chinese) **2013**, 1006–1012.
7 Li, Y.; Han, C. Y; Bian, Y. J.; Dong, Q. L.; Zhao, H. W.; Zhang, X.; Xu, M. Z.; Dong, L. S. Miscibility, thermal properties and polymorphism of stereocomplexation of high-molecular-weight polylactide/poly(D,L-lactide) blends. *Thermochim. Acta* **2014**, *580*, 53–62.
8 Tsuji, H. In vitro hydrolysis of blends from enantiomeric poly(lactide)s. Part 4: well-homo-crystallized blend and nonblended films. *Biomaterials* **2003**, *24*, 537–547.
9 Tsuji, H.; Hyon, S. H.; Ikada, Y. Stereocomplex formation between enantimoeric poly(lactides)s. 3. Calorimetric studies on blend

films cast from dilute solution. *Macromolecules* **1991**, *24*, 5651–5656.
10 Tsuji, H. Poly(lactide) stereocomplexes: formation, structure, properties, degradation, and applications. *Macromol. Biosci.* **2005**, *5*, 569–597.
11 Hirata, M.; Kimura, Y. Thermo mechanical properties of stereoblock poly(lactic acid)s with different PLLA/PDLA block compositions. *Polymer* **2008**, *49*, 2656–2661.
12 Fukushima, K.; Kimura, Y. Stereocomplexed polylactides (Neo-PLA) as high-performance bio-based polymers: their formation, properties, and application. *Polym. Int.* **2006**, *55*, 626–642.
13 Yang, S.; Zhong, G. J.; Xu, J. Z.; Li, Z. M. Preferential formation of stereocomplex in high-molecular-weight polylactic acid racemic blend induced by carbon nanotubes. *Polymer* **2016**, *105*, 167–171.
14 Tsuji, H.; Yamamoto, S. Enhanced stereocomplex crystallization of biodegradable enantiomeric poly(lactic acid)s by repeated casting. *Macromol. Mater. Eng.* **2011**, *296*, 583–589.
15 Han, L.; Pan, P.; Shan, G.; Bao, Y. Stereocomplex crystallization of high-molecular-weight poly(L-lactic acid)/poly(D-lactic acid) racemic blends promoted by a selective nucleator. *Polymer* **2015**, *63*, 144–153.
16 Xie, Q.; Han, L. L.; Shan, G. R.; Bao, Y. Z.; Pan, P. J. Promoted stereocomplex formation and two-step crystallization kinetics of poly(L-lactic acid)/poly(D-lactic acid) blends induced by nucleator. *Polym. Crystal.* **2019**, *2*, e10057.
17 Xie, Q.; Han, L. L.; Shan, G. R.; Bao, Y. Z.; Pan, P. J. Polymorphic crystalline structure and crystal morphology of enantiomeric poly(lactic acid) blends tailored by a self-assemblable aryl amide nucleator. *ACS Sustain. Chem. Eng.* **2016**, *4*, 2680–2688.
18 Urayama, H.; Kanamori, T.; Fukushima, K.; Kimura, Y. Controlled crystal nucleation in the melt-crystallization of poly(L-lactide) and poly(L-lactide)/poly(D-lactide) stereocomplex. *Polymer* **2003**, *44*, 5635–5641.
19 Xiong, Z. J.; Zhang, X. Q.; Wang, R.; de Vos, S.; Wang, R. Y.; Joziasse, C. A. P.; Wang, D. J. Favorable formation of stereocomplex crystals in poly(L-lactide)/poly(D-lactide) blends by selective nucleation. *Polymer* **2015**, *76*, 98–104.
20 Girdthep, S.; Sankong, W.; Pongmalee, A.; Saelee, T.; Punyodom, W.; Meepowpan, P.; Worajittiphon, P. Enhanced crystallization, thermal properties, and hydrolysis resistance of poly(l-lactic acid) and its stereocomplex by incorporation of graphene nanoplatelets. *Polym. Test.* **2017**, *61*, 229–239.
21 Huang, Y. F.; Zhang, Z. C.; Li, Y.; Xu, J. Z.; Xu, L.; Yan, Z.; Zhong, G. J.; Li, Z. M. The role of melt memory and template effect in complete stereocomplex crystallization and phase morphology of polylactides. *Cryst. Growth Des.* **2018**, *18*, 1613–1621.
22 Zhang, J. M.; Tashiro, K.; Tsuji, H.; Domb, A. J. Investigation of phase transitional behavior of poly(L-lactide)/poly(D-lactide) blend used to prepare the highly-oriented stereocomplex. *Macromolecules* **2007**, *40*, 1049–1054.
23 Pan, G. W.; Xu, H. L.; Mu, B. N.; Ma, B. M.; Yang, J.; Yang, Y. Q. Complete stereo-complexation of enantiomeric polylactides for scalable continuous production. *Chem. Eng. J.* **2017**, *328*, 759–767.
24 Feng, C. S; Chen, Y.; Shao, J.; Hou, H. Q. The crystallization behavior of poly(l-lactic acid)/poly(d-lactic acid) electrospun fibers: Effect of distance of isomeric polymers. *Ind. Eng. Chem. Res.* **2020**, *59*, 8480–8491.
25 Biela, T.; Duda, A.; Penczek, S. Enhanced melt stability of star-shaped stereocomplexes as compared with linear stereocomplexes. *Macromolecules* **2006**, *39*, 3710–3713.
26 Sun, Y.; He, C. Synthesis and stereocomplex crystallization of poly(lactide)-graphene oxide nanocomposites. *ACS Macro Lett.* **2012**, *1*, 709–713.
27 Liu, Y. L.; Sun, J. R.; Bian, X. C.; Feng, L. D.; Xiang, S.; Sun, B.; Chen, Z. M.; Li, G.; Chen, X. S. Melt stereocomplexation from poly(l-lactic acid) and poly(d-lactic acid) with different optical purity. *Polym. Degrad. Stabil.* **2013**, *98*, 844–852.
28 Bao, R. Y.; Yang, W.; Jiang, W. R.; Liu, Z. Y.; Xie, B. H.; Yang, M. B.; Fu, Q. Stereocomplex formation of high-molecular-weight polylactide: a low temperature approach. *Polymer* **2012**, *53*, 5449–5454.
29 Bai, D. Y.; Liu, H. L.; Bai, H. W.; Zhang, Q.; Fu, Q. Powder metallurgy inspired low-temperature fabrication of high-performance stereocomplexed polylactide products with good optical transparency. *Sci. Rep.* **2016**, *6*, 20260.
30 Bai, D. Y.; Liu, H. L.; Bai, H. W.; Zhang, Q.; Fu, Q. Low-temperature sintering of stereocomplex-type polylactide nascent powder: effect of crystallinity. *Macromolecules* **2017**, *50*, 7611–7619.
31 Purnama, P.; Kim, S. H. Stereocomplex formation of high-molecular-weight polylactide using supercritical fluid. *Macromolecules* **2010**, *43*, 1137–1142.
32 Zhang, Z. C.; Sang, Z. H.; Huang, Y. F.; Ru, J. F.; Zhong, G. J.; Ji, X.; Wang, R.; Li, Z. M. Enhanced heat deflection resistance *via* shear flow-induced stereocomplex crystallization of polylactide systems. *ACS Sustain. Chem. Eng.* **2017**, *5*, 1692–1703.
33 Song, Y.; Zhang, X. Q.; Yin, Y. A.; de Vos, S.; Wang, R. Y.; Joziasse, C. A. P.; Liu, G. M.; Wang, D. J. Enhancement of stereocomplex formation in poly(L-lactide)/poly(D-lactide) mixture by shear. *Polymer* **2015**, *72*, 185–192.
34 Ju, Y. L.; Li, X. L.; Diao, X. Y.; Bai, H. W.; Zhang, Q.; Fu, Q. Mixing of racemic poly(L-lactide)/poly(D-lactide) blend with miscible poly(D,L-lactide): toward all stereocomplex-type polylactide with strikingly enhanced SC crystallizability. *Chinese J. Polym. Sci.* **2021**, *39*, 1470–1480.
35 Bao, R. Y.; Yang, W.; Liu, Z. Y.; Xie, B. H.; Yang, M. B. Polymorphism of a high-molecular-weight racemic poly(l-lactide)/poly(d-lactide) blend: effect of melt blending with poly(methyl methacrylate). *RSC Adv.* **2015**, *5*, 19058–19066.
36 Bao, R. Y.; Yang, W.; Wei, X. F.; Xie, B. H.; Yang, M. B. Enhanced formation of stereocomplex crystallites of high molecular weight poly(L-lactide)/poly(D-lactide) blends from melt by using poly(ethylene glycol). *ACS Sustain. Chem. Eng.* **2014**, *2*, 2301–2309.
37 Pan, P. J.; Bao, J. N.; Han, L. L.; Xie, Q.; Shan, G. R.; Bao, Y. Z. Stereocomplexation of high-molecular-weight enantiomeric poly(lactic acid)s enhanced by miscible polymer blending with hydrogen bond interactions. *Polymer* **2016**, *98*, 80–87.
38 Loomis, G. L.; Murdoch, J. R.; Gardner, K. H. Polylactide stereocomplexs. *Polym. Prepr.* **1990**, *200*, 55.
39 Fischer, E. W.; Sterzel, H. J.; Wegner, G. Investigation of structure of solution grown crystals of lactide copolymers by means of chemical-reations. *Collid Polym. Sci.* **1973**, *251*, 980–990.
40 Zhang, J.; Tashiro, K.; Tsuji, H.; Domb, A. J. Disorder-to-order phase transition and multiple melting behavior of poly(L-lactide) investigated by simultaneous measurements of WAXD and DSC. *Macromolecules* **2008**, *41*, 1352–1357.
41 Wang, L.; Feng, C. S.; Zhou, D. D.; Shao, J.; Hou, H. Q.; Li, G. The crystallization and phase transition behaviors of asymmetric PLLA/PDLA blends: from the amorphous state. *Polym. Cryst.* **2018**, *1*, e10006.
42 Shao, J.; Sun, J. R.; Bian, X. C.; Zhou, Y. C.; Li, G.; Chen, X. S. The formation and transition behaviors of the mesophase in poly(d-lactide)/poly(l-lactide) blends with low molecular weights. *CrystEngComm* **2013**, *15*, 6469–6476.
43 Cartier, L.; Okihara, T.; Lotz, B. Triangular polymer single crystals: Stereocomplexes, twins, and frustrated structures. *Macromolecules* **1997**, *30*, 6313–6322.
44 Guo, Y. M.; Shao, J.; Hou, H. Q. The toughening behavior of PLLA

https://doi.org/10.1007/s10118-023-2901-y

and its asymmetric PLLA/PDLA blends with lower optical purity. *J. Appl. Polym. Sci.* **2017**, *134*, 44730.
45 Guo, Y. M.; Wang, L. Y.; Cheng, D. H.; Shao, J.; Hou, H. Q. Toughening behavior of poly(l-lactic acid)/poly(d-lactic acid) asymmetric blends. *Polym. Plast. Technol. Eng.* **2018**, *57*, 1225–1235.
46 Liu, Z. W.; Fu, M. R.; Ling, F. W.; Sui, G. P.; Bai, H. W.; Zhang, Q.; Fu, Q. Stereocomplex-type polylactide with bimodal melting temperature distribution: Toward desirable melt-processability and thermomechanical performance. *Polymer* **2019**, *169*, 21–28.
47 Shao, J.; Xu, L. L.; Pu, S. Z.; Hou, H. Q. The crystallization behavior of poly(l-lactide)/poly(d-lactide) blends: Effect of stirring time during solution mixing. *Polym. Bull.* **2021**, *78*, 147–163.
48 Chen, Y.; Hua, W. Q.; Zhang, Z. C.; Xu, J. Z.; Bian, F. G.; Zhong, G. J.; Xu, L.; Li, Z. M. An efficient, food contact accelerator for stereocomplexation of high-molecular-weight poly(l-lactide)/poly(d-lactide) blend under nonisothermal crystallization. *Polymer* **2019**, *170*, 54–64.
49 Zhang, J. M.; Sato, H.; Tsuji, H.; Noda, I.; Ozaki, Y. Infrared spectroscopic study of CH_3-O=C interaction during poly(L-lactide)/poly(D-lactide) stereocomplex formation. *Macromolecules* **2005**, *38*, 1822–1828.
50 Li, Z. L.; Zhang, M.; Fan, X.; Ye, X.; Zeng, Y.; Zhou, H. J.; Guo, W. J.; Ma, Y.; Shao, J.; Yan, C. Hydrogen bonding assists stereocomplexation in poly(l-lactic acid)/poly(d-lactic acid) racemic blends. *J. Polym. Sci., Part B: Polym. Phys.* **2019**, *57*, 83–88.
51 Yang, C. F.; Huang, Y. F.; Ruan, J.; Su, A. C. Extensive development of precursory helical pairs prior to formation of stereocomplex crystals in racemic polylactide melt mixture. *Macromolecules* **2012**, *45*, 872–878.
52 Feng, L. D.; Bian, X. C.; Li, G.; Chen, X. S. Thermal properties and structural evolution of poly(l-lactide)/poly(d-lactide) blends. *Macromolecules* **2021**, *54*, 10163–10176.
53 Feng, L. D.; Bian, X. C.; Li, G.; Chen, X. S. Compatibility and thermal and structural properties of poly(l-lactide)/poly(l-*co*-d-lactide) blends. *Macromolecules* **2022**, *55*, 1709–1718.

https://doi.org/10.1007/s10118-023-2901-y